Characterizing the microstructural and architectural organization of healthy kidney tissue using diffusion tensor imaging, fiber tractography and intra-voxel incoherent motion.

Sophie van Baalen[1], Alexander Leemans[2], Pieter Dik[1], Bennie ten Haken[3], and Martijn Froeling[2]
[1]*Pediatric Urology, University Medical Centre Utrecht/ WKZ, Utrecht, Netherlands,* [2]*Imaging science institute, University Medical Centre Utrecht, Utrecht, Netherlands,* [3]*Institute for Biomedical Technology and Technical Medicine, University of Twente, Enschede, Netherlands*

Introduction: Diffusion tensor imaging (DTI) can determine the direction and extent of water diffusion in renal tissue, as recent studies have shown [1-4]. Additionally, intra-voxel incoherent motion (IVIM) is a method that allows for the measurement of the perfusion fraction in tissue [5,6] and has been applied to several abdominal organs[7] and kidney tumors[8]. An important advantage of these techniques is that they make no use of contrast agents that can be harmful for renal patients. In this study, a combination of DTI with fiber tractography and IVIM was used to visualize the microstructural architecture of healthy kidney tissues. This enabled the characterization of multiple aspects of kidney tissue, including structural properties, blood perfusion fraction and urine diffusion fraction, without the use of contrast agents.

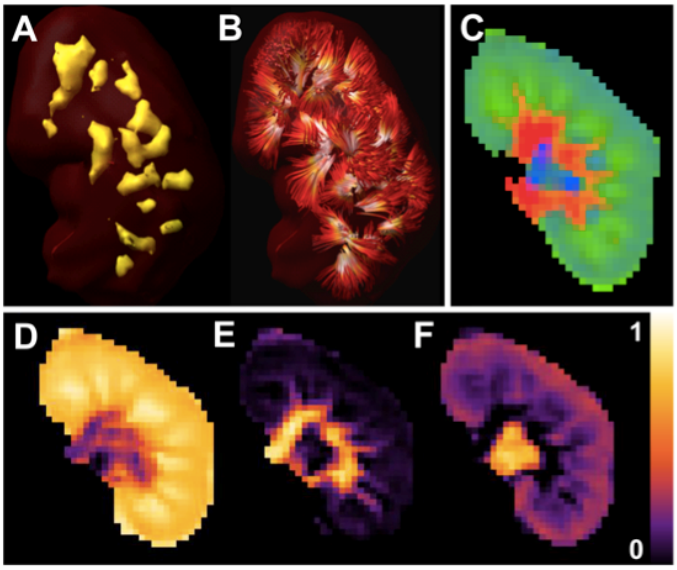

Figure 1 A: *tract density seeds (yellow) in kidney volume mask contour (red),* ***B****: tracts are radially oriented, originating in the cortex (red) and convolving in multiple papilla (white)* ***C:*** *combined map of diffusion fractions red: blood blue: urine green: tissue* ***D to F*** *Maps of diffusion fractions.* ***D:*** *tissue diffusion,* ***E:*** *Blood perfusion,* ***F:*** *urine diffusion*

Methods: MRI acquisition: Approval of our institution's ethical committee was obtained for this research. Ten healthy volunteers were scanned on a 3T Philips Intera clinical scanner. The volunteers underwent T2 TSE imaging (TE: 100ms, TR: 2418ms, Matrix size: 400x320, FOV: 450x450mm^2, voxel size: 1.13x1.41x3.0mm) as well as DTI (TE: 39ms, TR: 1267ms, Matrix size: 112x68, FOV: 336x204mm^2, voxel size: 3.0x3.0x3.0 mm, b-values: 0,100,300 s/mm^2, gradient directions: 15) and IVIM imaging (TE: 45ms, TR: 1344ms, Matrix size: 112x68, FOV: 336x204mm^2, voxel size: 3.0x3.0x3.0 mm, b-values: 0, 10, 25, 40, 75, 100, 200, 300, 500, 700 s/mm^2, gradient directions: 3). The DTI and IVIM acquisitions were respiratory triggered using a navigator. Diffusion weighted images were corrected for misalignments due to subject motion and eddy current induced geometric distortions[9].
Tractography: Whole-kidney tractography (seed FA threshold: 0.001, FA tracking threshold range: 0.1 – 0.5, MD tracking threshold range: 0.001-0.0035, angle threshold: 20) was performed after masking of the kidney volume using manually placed ROI's on each coronal slice, using "ExploreDTI"[10]. From the obtained fiber tracts a tract density map[11] was created which was used to construct seeds to select those groups of tracts that convolve in papillae (threshold: $\frac{Ntracts_{local}}{Ntracts_{max}} > 0.08$, see figure 1A).
IVIM: A tri-exponential fit was used to calculate the fractions of tissue diffusion, perfusion and urine diffusion:
$S_b = S_0 \frac{(1-f_b-f_u)* S_{tissue}*e^{-bD_t} + f_b*S_{blood}*e^{-bD_b^*} + f_u*S_{urine}*e^{-bD_u^*}}{(1-f_b-f_u)* S_{tissue} + f_b*S_{blood} + f_u*S_{urine}}$, in which f_b= perfusion fraction, f_u= urine diffusion fraction, $(1-f_b-f_u)$= tissue diffusion fraction, D_t= diffusion coefficient, D_b^*= pseudodiffusion coefficient of blood and D_b^*= pseudodiffusion coefficient of urine. S_{tissue}, S_{blood} and S_{urine} are the relative signal contributions based on the relaxation times of kidney tissue, blood and urine, respectively[12]. First, the mean signal of the whole kidney volume was used for a preliminary fit, calculating all parameters, f_b, f_u, D_t, D_b^* and D_u^*. Then, the calculated D_b^* and D_u^* were assumed constant over the whole kidney volume. Using the fixed values of D_b^* and D_u^*, a voxel by voxel calculation of the tissue fractions and D_t, was performed.

Results: Tractography: Tracts are radially oriented, originating in the cortex and convolving in multiple papillae in the renal center (see figure 1B). These tracts reflect the architectural configuration of the renal medulla, consisting of radially oriented straight tubules and vascular network.
IVIM: Figure 1C,D,E, and F show the tissue diffusion, blood perfusion, and urine diffusion fraction maps. Central to the kidney, perfusion fraction and urine fraction areas are consistent with known anatomy of renal vessels and pyelum, respectively. In addition, the fractions are more homogeneous in the renal medulla and cortex. The mean values for f_b, f_u, D_t, D_b^* and D_u^* from the whole-volume fit are summarized in table 1.

Tabel 1: *mean and standard deviation of parameters calculated with whole volume fit*

	f_b	f_u	D_t (10^{-3} mm^2/2)	D_b^* (10^{-3} mm^2/2)	D_u^* (10^{-3} mm^2/2)
Mean ± standard deviation	12%±3%	38% ± 12%	1.5±0.2	227±64	9.3±5.7

Conclusion: DTI with tractography is able to visualize the tissue architecture of the kidney, especially its renal pyramids, papillae, and major and minor calyxes. With IVIM, perfusion fraction, urine diffusion, and tissue diffusion can be characterized. Combined, these techniques can be a valuable tool for the diagnosis of many renal pathologies, including renal scarring, kidney tumors, and follow-up after kidney transplantation.

References: [1.] Notohamiprodjo, et al. *Invest. Radiol*. 2010;45:245–254.[2.] Hueper, et al. *Europ. Radiol*. 2011;21(11):2427–2433. [3.] Wu , et al. *Acad. Radiol*. 2011;18(9):1168–1174.[4.] Jaimes, et al. *Pediatr. Radiol*. 2013.[5.] Le Bihan et al. *Radiol*. 1986;161:401–407.[6.] Le Bihan *Radiol*. 1988;168:497–505. [7.] Sigmund, et al. *Radiol*. 2012;263(3):758–769. [8.] Chandarana, et al. *Invest. Radiol*. 2012;47(12):1–9.[9.] Leemans et al. *MRM,* 2009;61(6):1336–1349.[10.] Leemans et al. *ISMRM,* Hawaii, USA; 2009:3537. [11.] Calamante et al. *NeuroIm*. 2011;56(3):1259–1266.[12.] Lemke et al. *MRM,* 2010;64(6):1580–1585.